Geotech Geol Eng (2012) 30:331–342
DOI 10.1007/s10706-011-9471-4

ORIGINAL PAPER

Physical and Numerical Modeling of Seismic Soil-Structure Interaction in Layered Soils

M. T. Rayhani · M. H. El Naggar

Received: 9 September 2009 / Accepted: 15 October 2011 / Published online: 1 November 2011

Abstract The structural response of buildings subjected to seismic loads is affected by local site conditions and the interaction between the structure and the supporting soil media. Seismic centrifuge model tests were conducted on two layered clay soil profiles at 80 g field to investigate soil-structure interaction and dynamic response of foundation. Several earthquake-like shaking events were applied to the models using an electro-hydraulic shaking table to simulate linear and nonlinear soil behavior. Results showed that the foundation input motion was significantly amplified in both models, especially for weak earthquake motions. Seismic soil-structure interaction was found to have an important effect on structure response by increasing the amplification of foundation input motion. A 3D finite difference numerical model was also developed to simulate the response of centrifuge model tests and study the parameters that affect the characteristics of earthquake at the base of the structure. The results indicated that the stiffness and stratification of the soil profiles had a significant effect on modifying the foundation input motion.

Keywords Soil-structure interaction · Soil layering · Centrifuge test · Numerical model

M. T. Rayhani (✉)
Department of Civil and Environmental Engineering, Carleton University, Ottawa, Canada
e-mail: mrayhani@connect.carleton.ca

M. H. El Naggar
Department of Civil and Environmental Engineering, University of Western Ontario, London, ON N6A 5B9, Canada
e-mail: helnaggar@eng.uwo.ca

1 Introduction

Local site conditions have a significant influence in the distribution of damage associated to earthquake. Recent earthquakes like Kobe (1995), Northridge (1994), and Loma Prieta (1989) have depicted the role of local site conditions in changing the characteristics of the strong motion data. Site conditions influence the seismic response of structures by soil amplification/attenuation in which the bedrock motions are modified during transmission through the overlying soil. Local site conditions may generate large amplifications and significant spatial variations of seismic ground motion, and cause substantially different amounts of structural damage in the same general area (Sanchez-sesma 1987). On the other hand, soil-structure interaction (SSI) can significantly change the free field ground motion at the foundation level and the dynamic response of the structure (Veletsos and Prasad 1989).

High amplification of ground motion and severe damage to buildings in the 1989 Loma Prieta earthquake sequence suggested that the configuration,

thickness, and composition of the natural materials had a strong influence on shaking (Bonilla 1991). Ground failure at Malden Street in Los Angeles during the 1994 Northridge earthquake, which broke water lines and damaged foundations, is another example where the localised weak soils affected the overall dynamic response of the ground, probably by dynamic shear in weak clay (Holzer et al. 1999).

In the 1995 Kobe earthquake, the ground motions were amplified by a factor of 1.5–2 times in the heavily damaged areas within deep sedimentary layers, whereas in the reclaimed areas widespread liquefaction occurred and the measured peak accelerations were the same as those in the rock. This was attributed to the isolation effect of liquefied soil. This led to the conclusion that local site effects including those resulting from soil liquefaction was responsible for reducing the damage to superstructures particularly located near coast lines (Tokimatsu et al. 1996). It shows that having a liquefiable layer trapped between dense soil layers could be a possible remediation method against such amplification (Ghosh and Madabhushi 2003).

The effects of soil-structure interaction (SSI) and nonlinear site response (SR) on the Northridge main shock and aftershock motions recorded at two buildings in the Jensen Filtration Plant were investigated by Crouse and Ramirez (2003). Nonlinear SR and kinematic SSI were identified as the main reasons for the differences observed in the three sets of building earthquake records, each with clearly distinct amplitude and duration characteristics. However, models of inertial SSI, calibrated to the vibration test data, demonstrated that this phenomenon was of secondary importance, even when adjusted for nonlinear behavior of the soil and structure.

Aviles and Perez-Rocha (1997) investigated site effects and SSI during the Mexico earthquake of 1985. Based on their study, significant effects of SSI have been identified for medium and long period structures founded on soft soils. Interaction effects were found to be larger for tall and slender structures than for short and squat structures of the same period, and they decreased as the foundation depth increased.

Most code provisions recommend simplified model for SSI problem, which ignores significant characteristics of SSI and local site effect including nonlinear response and soil layering and inhomogeneity. However, they acknowledge the need for site specific studies for structures on soft soils subject to strong levels of shaking.

The objective of the research described in this paper is to evaluate the effect of soil stratification on the transmission characteristics of the ground motion and dynamic structural response. Seismic centrifuge testing of layered soft soil deposits was performed using a geotechnical centrifuge at the C-CORE testing facilities in Newfoundland. Numerical modeling verified by the centrifuge test results were used to study stratification effects on amplification of the foundation input motions. Seismic soil-structure interaction analysis was performed for earthquakes with different excitation levels and frequency contents through different soil profiles.

2 Centrifuge Modeling

Dynamic centrifuge model tests were conducted at 80-g on the C-CORE 5.5 m radius beam centrifuge located at Memorial University of Newfoundland. An electro-hydraulic earthquake simulator (EQS) was mounted on the centrifuge to apply a one-dimensional prescribed base input motion. A rigid shear beam model container with inner dimensions of 0.73 m in length, 0.3 m in width, and 0.57 m in height was employed to simulate shear beam boundary conditions for the soil. The centrifuge models comprised two layered soft to medium soil profiles with different configurations (RG-03, RG-04). The results were presented in prototype units unless otherwise noted.

2.1 Centrifuge Model Configuration

Model configuration of both soil profiles in centrifuge container is shown in Fig. 1. Model RG-03 soil model consisted of an intermediate medium stiff clay with shear strength of about 60 kPa with upper and lower layers of soft clay ($S_u = 30$ kPa). Model RG-04 consisted of lower and upper layers of medium stiff clay ($S_u = 60$ kPa) and an intermediate layer of soft clay ($S_u = 30$ kPa). The system models included a rigid structure and a mat foundation slightly embedded in the soil. The total thickness of the soil model was approximately 0.375 m, which simulates 30 m on prototype scale, based on scaling analysis proposed by Kutter (1194). The stress and strain have a scaling factor of '1' (Kutter and al 1994). Therefore, using the

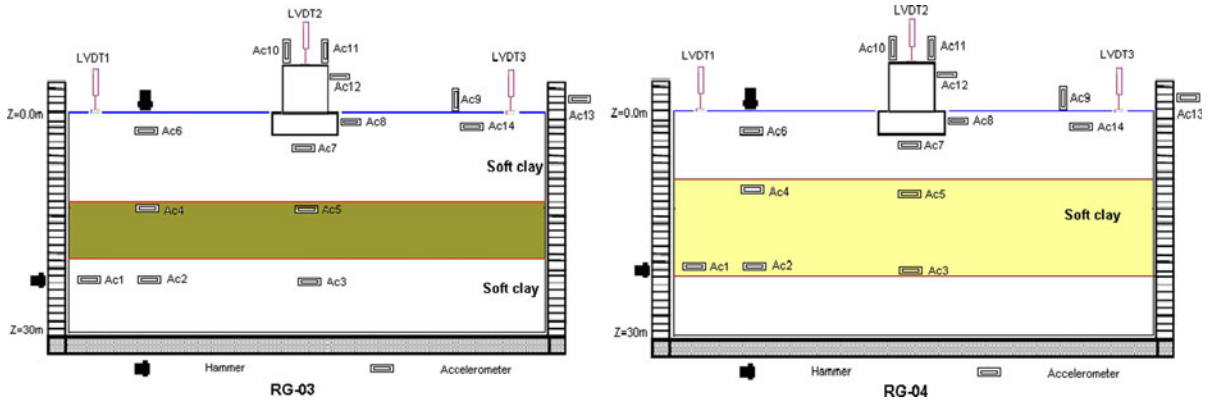

Fig. 1 Centrifuge model configuration in prototype scale

Table 1 Index properties of glyben samples

Liquid limit	Plastic limit	Plasticity index	Specific gravity	Density (kg/m^3)	Glycerin content (%)	Void ratio
50	39.5	10.5	2.73	1770	39	0.94

same material in the model and prototype and placing the model in centrifuge acceleration field 80 times normal terrestrial gravity results in the same stress and strains at homogeneous points. The resulting average bearing stress at 80 g beneath the structure model is 95 kPa. This stress represents a reasonable simulation for the load applied by a ten-storey building. All models were instrumented to measure free field and foundation accelerations, free field displacements, and local deformations on basement walls and foundation slabs. The models were subjected to earthquake excitations with different accelerations.

Glyben clay with glycerin ratios of 45 and 42.5% with undrained vane shear strengths of about 30–60 kPa was used here to simulate soft and medium stiff clay behavior in model tests. Table 1 presents the physical properties of optimum compaction glyben clay (Rayhani and El Naggar 2008a). Glycerin and bentonite were mixed at a ratio of 45%/55% for soft clay and 42.5%/57.5% for medium stiff clay. The models were prepared by tamping the soil in layers to obtain the desired void ratio (90% of maximum dry density). The homogeneity of each clay layer was checked by conducting vane shear tests at depth intervals of 50 mm. The variations of shear strength were less than 5% for each layer, which shows reasonable uniformity in samples.

Accelerometers were used to measure the soil acceleration at different depths and the structure accelerations. The accelerometers were placed within the soil bed by tamping the glyben to the required level, placing the instrument in the desired position and then adding more soil to the required level. There were also accelerometers on top of the structure and on its walls. The system model was also instrumented with Linear Variable Differential Transducers (LVDTs) to measure the settlement of the soil surface and the vertical displacement of the model structure. For measurement of free field settlements, the extenders from the core of LVDTs rested against tin disks, approximately 10 mm in diameter.

Estimating the soil shear strength profile is very important in site response and soil-structure interaction analyses, especially for large strain and nonlinear soil response. In the model soils, the applied seismic and structure loadings could be expected to generate undrained stress–strain soil response, and it was therefore necessary to evaluate the undrained shear strength of the model soil. T-bar tests were performed at 80 g to determine a continuous profile of the deposit undrained shear strength, S_u. The T-bar was 31 mm wide and 7.9 mm in diameter and was pushed into the soil at a rate of approximately 3 mm/s. The results were interpreted using the plasticity solution for the limiting pressure

acting on a cylinder moving laterally through purely cohesive soil, which gives the limiting force acting on the cylinder as (Randolph and Houlsby 1984):

$$S_u = {}^{P}/_{N_b d} \quad (1)$$

where P is force per unit length acting on the cylinder, d is the diameter of cylinder and N_b is the bar factor. The factor N_b of the T-bar was considered equal to 10.5 in the interpretation of the results (Rayhani and El Naggar 2008a). Figure 2(a) shows the T-bar results in the centrifuge container at 80 g for both test models. The shear strength for model RG-03 were measured about 40–50 kPa and 60–65 kPa for soft and medium stiff clay, respectively, and for model RG-04 about 48–52 kPa to 60–75 kPa for soft and medium stiff clay, respectively. The shear strength increased slightly with depth (i.e. with confining pressure) wihthin each layer.

The shear wave velocity profile at different depths was estimated using established relation between shear strength and shear wave velocity for glyben clay (Rayhani and El Naggar 2008a). This relation was proposed based on the measured undrained shear strength, S_u, and measured shear wave velocity in resonant column tests. As it can be seen from Fig. 2(b), the shear wave velocity gradually increased with depth, within each layer, in both models. The shear wave velocity varied between 60 and 70 m/s for soft layers and between 75 and 85 m/s for medium stiff layers in both models. The mean shear wave velocity was estimated about 65 and 73 m/s for models RG-03 and RG-04, respectively.

Three levels of earthquake excitation were desired for the soil-structure scale model tests. Two low level accelerations with a PHA of 0.07–0.1 g were targeted to ensure that response remained in the elastic range. Two mid range signal with a PHA of about 0.18–0.22 g were desired to impart an intermediate level excitation. Finally, two strong shaking record with a PHA 0.39–0.54 g were sought to induce nonlinear site and structure response, typical of design level events in regions of high seismicity. The earthquake motions were applied using the electro-hydraulic simulator described by Coulter and Phillips (2003). Table 2 shows the input excitations, i.e. scaled versions of an artificial Western Canada Earthquake (Seid-Karbasi 2003) and the actual recordings of the Port Island downhole array −79 m record north-east component from the Kobe earthquake. The test data was collected using a high-speed data acquisition system.

2.2 Test Results

Table 2 lists peak accelerations at different locations for all shaking events (see Fig. 1): Peak accelerations generally increased from base to surface. The peak horizontal acceleration near the surface ranged from 0.12 to 0.57 g for model RG-03 and from 0.14 to 0.56 g for model RG-04. This range of peak acceleration covered both linear and nonlinear response scenarios. The peak accelerations of the structure were 10–30% greater than the values measured at the soil beneath the structure. The free field accelerations were slightly less than those beneath the structure in both models.

The settlement of soil surface was measured using LVDTs attached to the model racks and extended

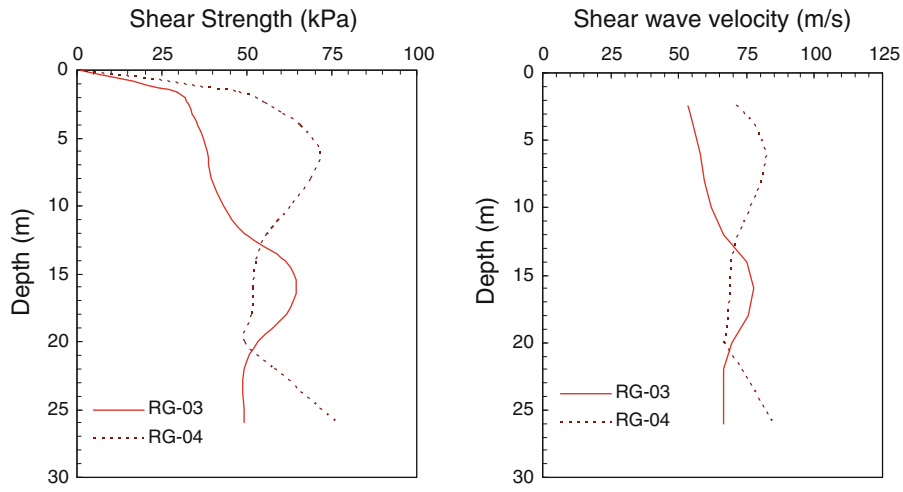

Fig. 2 Shear strength and shear wave velocity profile for both models at 80 g

Table 2 Shaking events and peak accelerations (units in prototype scale, g)

Model	Event	Base acc.	A2	A3	A4	A5	A6	A7	A8	A12
RG-03	WCL	0.1	0.12	0.12	0.13	0.135	0.15	0.17	0.18	0.19
	WCM	0.18	0.21	0.21	0.2	0.21	0.23	0.26	0.27	0.29
	WCH	0.36	0.36	0.36	0.36	0.356	0.39	0.41	0.415	0.45
	KL	0.07	0.09	0.09	0.1	0.1	0.12	0.14	0.15	0.165
	KM	0.22	0.25	0.25	0.26	0.28	0.3	0.34	0.35	0.38
	KH	0.49	0.5	0.53	0.47	0.495	0.53	0.57	0.575	0.62
RG-04	WCL	0.1	0.12	0.12	0.155	0.17	0.16	0.175	0.175	0.18
	WCM	0.18	0.2	0.2	0.24	0.255	0.235	0.275	0.275	0.29
	WCH	0.36	0.35	0.34	0.375	0.36	0.37	0.4	0.42	0.46
	KL	0.07	0.1	0.09	0.14	0.145	0.14	0.16	0.17	0.18
	KM	0.22	0.27	0.24	0.32	0.33	0.33	0.37	0.38	0.39
	KH	0.49	0.53	0.54	0.56	0.59	0.56	0.64	0.66	0.74

WCL Western Canada (weak), *WCM* Western Canada (moderate), *WCH* Western Cnada (strong), *KL* Kobe (weak), *KM* Kobe (moderate), *KH* Kobe (strong)

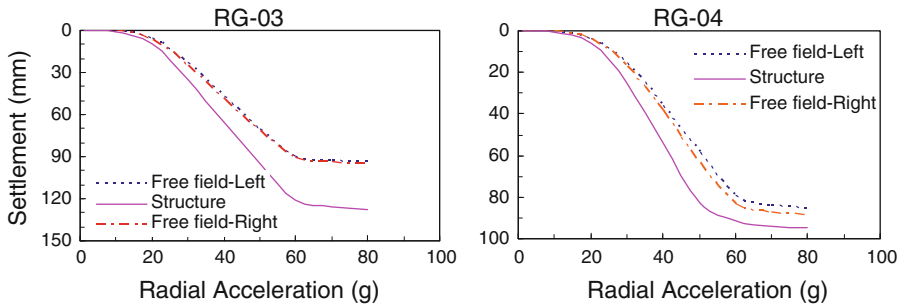

Fig. 3 Settlements curves from 1–80 g, before shaking in prototype scale

downward to pads placed at the soil surface. In order to measure structural settlement, an LVDT was used on top of the structure. Figure 3 depicts the swing-up settlement curves from 1 to 80 g for the free field and structure in prototype scale. The maximum settlement of the clay models varied from 70 to 90 mm for RG-04 and up to about 140 mm for RG-03 models, which is similar to those recorded for natural soft clays (e.g. Fox et al. 2005). However, the vast majority of settlement occurred as the model swung up from 1 to 80 g. This initial (almost immediate) settlement is attributed to compaction of glyben. The settlement measured as the model spun at 80 g until testing started was negligible and was attributed to consolidation. The rate of consolidation, however, was much smaller than for natural and artificial clays (e.g. Bransby et al. 2001) such that consolidation during testing was negligible and the stress–strain behavior was considered to be undrained.

3 Experimental Data Analysis

3.1 Amplification of Free Field Motion

Amplification of free field motions were evaluated from three accelerometers placed along a vertical plane far from the structure, and a similar setup was used to evaluate the amplification beneath the structure. Figure 4 shows acceleration amplification with depth for all shaking events. The amplification factors were obtained by normalizing the peak recorded acceleration at a given elevation by the corresponding peak acceleration of the base excitation. It can be inferred that the soil stiffness and layering greatly impacted the characteristics of the ground motion through the soil profile. For model RG-03, the surface amplification factor was 1.7–1.07 for events KL ($a_{max} = 0.07$ g) and KH ($a_{max} = 0.49$ g), respectively. For model RG-04, this factor varied from

1.03 for KH to 2.0 for event KL. It is interesting to note that most of the amplification occurred in the soft clay layers, especially for low earthquake motions. This observation underscores the importance of considering the soil layering when evaluating the free field motion and not just the average of shear wave velocity in the top 30 m of the soil profile. This is also highlighted by the low amplification in the KH and WCH events, which is attributed to softening of the soft clay as the stress level increased. The amplification factor decreased for stronger shaking events in all soil profiles. This reduction was attributed to nonlinear soil behaviour in higher amplitudes of motions. Also, higher peak amplitude of the ground acceleration and strain levels in the soil is associated with higher material damping which further reduces the response.

3.2 Seismic Soil-Structure Interaction

Three piezo-resistive accelerometers (model 3022-005g) were located beneath the structure along a vertical plane; one accelerometer was placed beside the structure in foundation level; and one accelerometer attached to the building wall to study the soil-structure interaction effect on ground motion. Spectral analysis was employed to characterize the frequency content of the input motion imposed on the structure and establish the predominant frequency of the earthquake loading. The transfer function of the site response (RRS) was used to assess the ground motion amplification and seismic hazard associated with different period earthquakes. Figure 5 shows the ratio of response spectra (RRS) curves or transfer functions, obtained by normalizing the acceleration response near the ground surface by those of the base. In general, the maximum values of RRS for beneath the structure were higher than those for the free field. This relative increase was about 10–20% for all earthquake events, which could be due to the structure feedback and strong interaction (kinematic) between the soil and foundation during shaking.

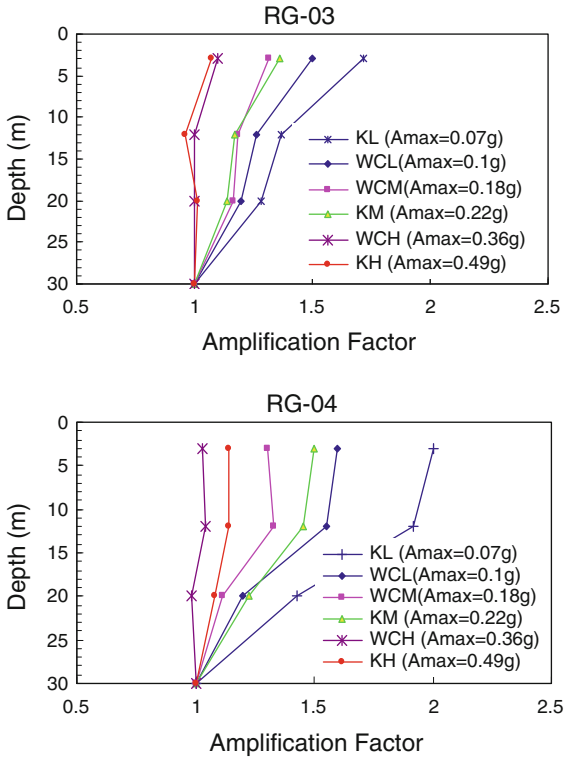

Fig. 4 Free field amplification with depth for all shaking events in both models

The variation of maximum RRS with base shaking amplitudes is shown in Fig. 6. The maximum RRS decreased in both soil models as the earthquake intensity increased. The peak RRS beneath the structure was higher than those for the free field, which shows the strong soil-structure interaction effects on foundation input motion. The difference between these values in model RG-03 was higher than RG-04, indicating more significant effect of SSI in softer layers. The reduction in maximum RRS for stronger shakings is attributed to the soil nonlinear response and its limited ability to transfer stresses to upper layers as the strength of the soil was reached. The progressive degradation of soil stiffness due to the cyclic shear strain amplitude could soften the soil (Ghosh and Madabhushi 2003). Thus, the system may undergo resonance at lower shakings while the higher shakings is being attenuated. Furthermore, at high strain levels the soil material damping increases as the earthquake amplitude increases, further reducing the response.

The inertial soil-structure interaction was evaluated by comparing readings from accelerometer A12 (attached to the structure wall) with accelerometer A8 (adjacent to the foundation). It is noted that A12 experienced higher acceleration (10–20%) compared to both A14 and A8 for both models, suggesting the effect of inertial SSI on structural behaviour (Table 2). The relative increase of structural acceleration was larger for stronger earthquake events (KH) which

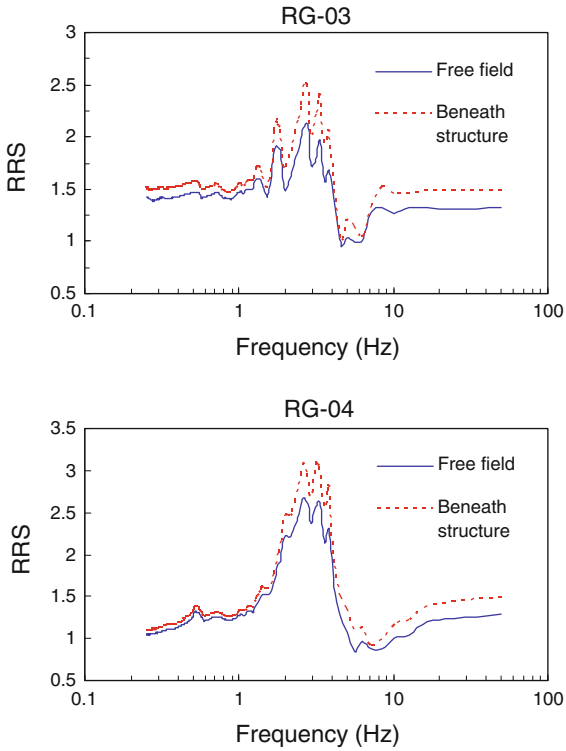

Fig. 5 Ratio of surface response to the base response spectra during the WCM event

could be due to the structure feedback and strong interaction between the soil and structure during shaking.

3.3 Structural Behaviour

The structural response was recorded by horizontal accelerometers A8 embedded in soil adjacent to the structure and A12 attached to the building wall. Vertical accelerometers were also attached to the structure top on both sides to measure possible rocking behavior. Absolute displacements of different points were obtained by integrating the measured accelerations, and relative movement of different points were obtained by subtracting their respective absolute displacements. The maximum relative lateral displacement of the structure is plotted in Fig. 7 for all shaking events. It can be noted that the movement of structure was negligible, but increased with the level of shaking. For example, for the KL event it was about 0.1 mm (prototype scale) for both models, and for the KH the calculated values were 1.3–1.8 mm. The relative lateral movement for RG-03, at stronger shaking levels, was higher than that for RG-04, which could be attributed to high nonlinearity in top soft layer.

Permanent settlement of the structure was evaluated from LVDT measurements at the end of each earthquake loading and is shown in Fig. 8. The maximum settlement during the earthquake excitations varied from 39 mm for RG-04 to about 41 mm for RG-03, in prototype scale. This settlement could be due to yielding of clay layers during earthquake excitations.

4 Numerical Modeling

4.1 Numerical Approach and Model Properties

A 3-D finite-difference-based program, *FLAC3D* (Itasca Consulting Group 2005), was used to develop the numerical model for the centrifuge model tests and to simulate their response under seismic loading. The Mohr–Coulomb plasticity constitutive model was used to simulate the nonlinear soil behavior. The failure envelope for this model corresponds to a Mohr–Coulomb criterion (shear yield) with tension cutoff (tension yield function). The modeling effort was focused on matching the observed test results. Therefore, the model parameters were defined to allow

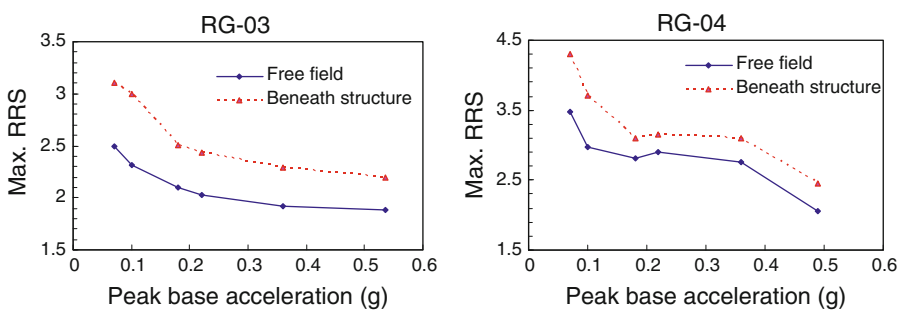

Fig. 6 Peak RRS for all shaking events in both models

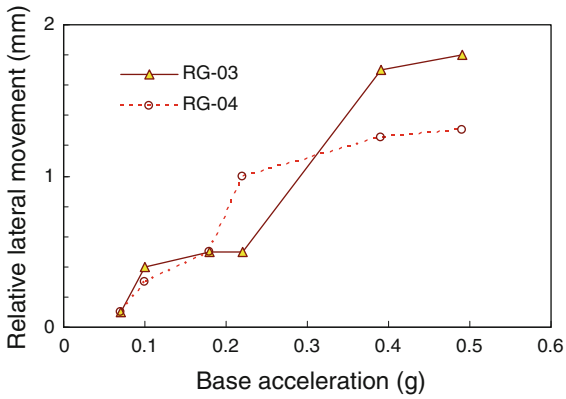

Fig. 7 Relative lateral movement of the structural for all shaking events

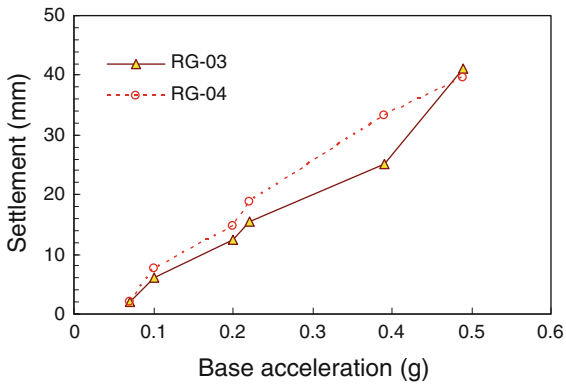

Fig. 8 Permanent settlement of structure for all shaking events

for a numerical response representative of that observed in centrifuge tests.

The soil profile was modeled with continuum zones, and the building was assumed to be rigid, which modeled the rigid aluminum foundation in the centrifuge model tests. Figure 9 shows the finite difference grid used in the *FLAC* model for the soil-structure system. The mesh size and the maximum unbalanced force at the grid points (i.e., error tolerance) were selected on the basis of a series of parametric analyses to concurrently optimize accuracy and computation speed. A fixed boundary condition in the vertical and y directions was assumed at the numerical grid points on the soil side boundaries, representing the centrifuge container that was used to contain the soil at the sides of the model test.

Dynamic soil properties calculated from the centrifuge test results and verified by the resonant column tests (Rayhani and El Naggar 2008a) were used to match with hysteretic damping parameters for nonlinear analysis in *FLAC*. Adequacy of the matching process was based on inspection of the recorded and computed shear modulus and damping at all shear strain ranges. Table 3 lists the main model parameters for both soil strata. The interfaces between the foundation and soil were modeled as linear spring–slider systems, with interface shear strength defined by the Mohr–Coulomb failure criterion. The preliminary interface stiffness components were estimated based on recommended rule-of-thumb estimates for maximum interface stiffness values given by Itasca Consulting Group _2005 (ten times the equivalent stiffness of the neighbouring zone), and then these values were adjusted by refining the magnitude of k_n and k_s to avoid intrusion of adjacent zones (a numerical effect) and to prevent excessive computation time. A reduced value of the soil cohesion was used for the interface cohesion (i.e., $c_{sf} = 30$ kPa in Table 3).

4.2 Simulation Results

Representative simulation results of the WCM event for model RG-03 at different depths are shown in Fig. 10, in terms of acceleration time histories and the corresponding response spectra (5% damping) along the soil profile. The numerical model shows an overall satisfactory match to the experimental results at all accelerometer locations, both in the time and frequency domains. This confirms that the overall damping of the model (hysteretic plus Rayleigh) represented the experimental damping behavior. Similar to the observed behavior in experiments, the computed response indicated that the seismic waves were amplified as they propagated from the bedrock to the surface. However, the calculated response spectra for periods ranging from 0.2 to 0.5 s were slightly less than the measured response spectra, for the region close to surface in both free field and underneath the structure. This may be attributed to the approximate modeling of the rigid boundaries (i.e. container) around the soil mass, and the soil-foundation interface parameters. The effect of boundary condition on dynamic response of structure has been presented by Rayhani and El Naggar (2008b).

4.3 Numerical Parametric Analysis

The characteristics of the foundation input motion are affected by the properties of the underlying soil

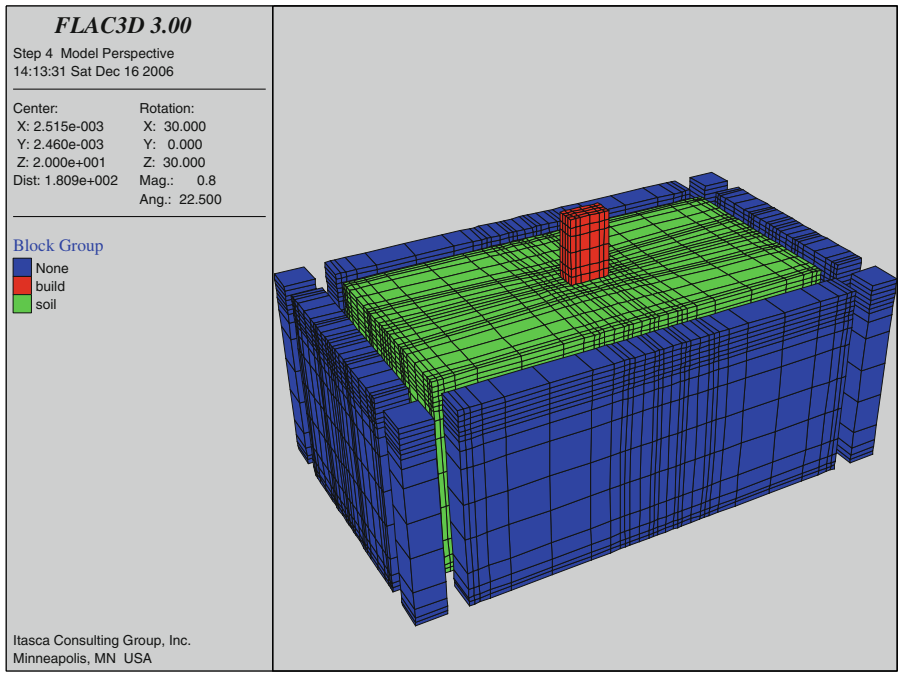

Fig. 9 Numerical grid and model component

Table 3 Major modeling properties of soft and medium stiff clay

Model parameters	Soft clay	Medium stiff clay
ρ, Mass density (kg/m^3)	1,575	1,595
k, Bulk modulus (kPa)	5.7×10^4	9.37×10^4
G, Shear modulus (kPa)	8.4×10^3	15.9×10^3
υ, Poisson's ratio (kPa)	0.43	0.42
E, Elastic modulus (kPa)	2.4×10^4	4.5×10^4
c, Cohesion intercept (kPa)	45	90
Interface properties		
c_{sb}, Cohesion (kPa)	30	45
k_n, Normal stiffness (kPa/m)	4.5×10^4	7.6×10^4
k_s, Shear stiffness (kPa/m)	5×10^2	8×10^2

through soil amplification and soil-structure interaction phenomena. Parametric studies were performed to evaluate the effects of soil layering and SSI on earthquake motion at the base of a structure, considering different soil profiles and different types of earthquake input motions.

4.3.1 *Effect of SSI on Foundation Input Motion*

The effect of soil-structure interaction (kinematic) on foundation input motion is assessed by comparing the free field motion and the foundation input motion (FIM). The deviation of the foundation input motion from the free-field motion is dependent on the stiffness and geometry of the foundation and soil properties. This deviation is expressed by a transfer function that represents the ratio of foundation and free-field motions in the frequency domain. Figure 11 shows the response spectra ratio of underneath the structure to the free field ($SA_{FIM}/SA_{Free\ field}$) in model RG-03. As it can be seen, the foundation accelerations are up to 27 percent higher than the free field over the frequency range of 2 Hz to 6 Hz. This behaviour is similar to estimated soil-structure interaction effects which have been identified by Aviles and Perez-Rocha (1997) for structures located on soft soils in Mexico City during the Mexico earthquake of 1985. These differences are most pronounced for the WCL and WCM shaking events. The difference between the free field ground motion and the foundation input motion (at the same level) is not significant at frequencies less than 2 Hz (5–9%). The parametric analyses indicated that the seismic soil-structure interaction, for the range of soil parameters considered here, has unfavorable effects on horizontal ground motions for frequencies between 2 and 6 Hz.

In order to investigate the effect of layering on seismic soil structure interaction, a series of analysis was performed on uniform soil profile with average

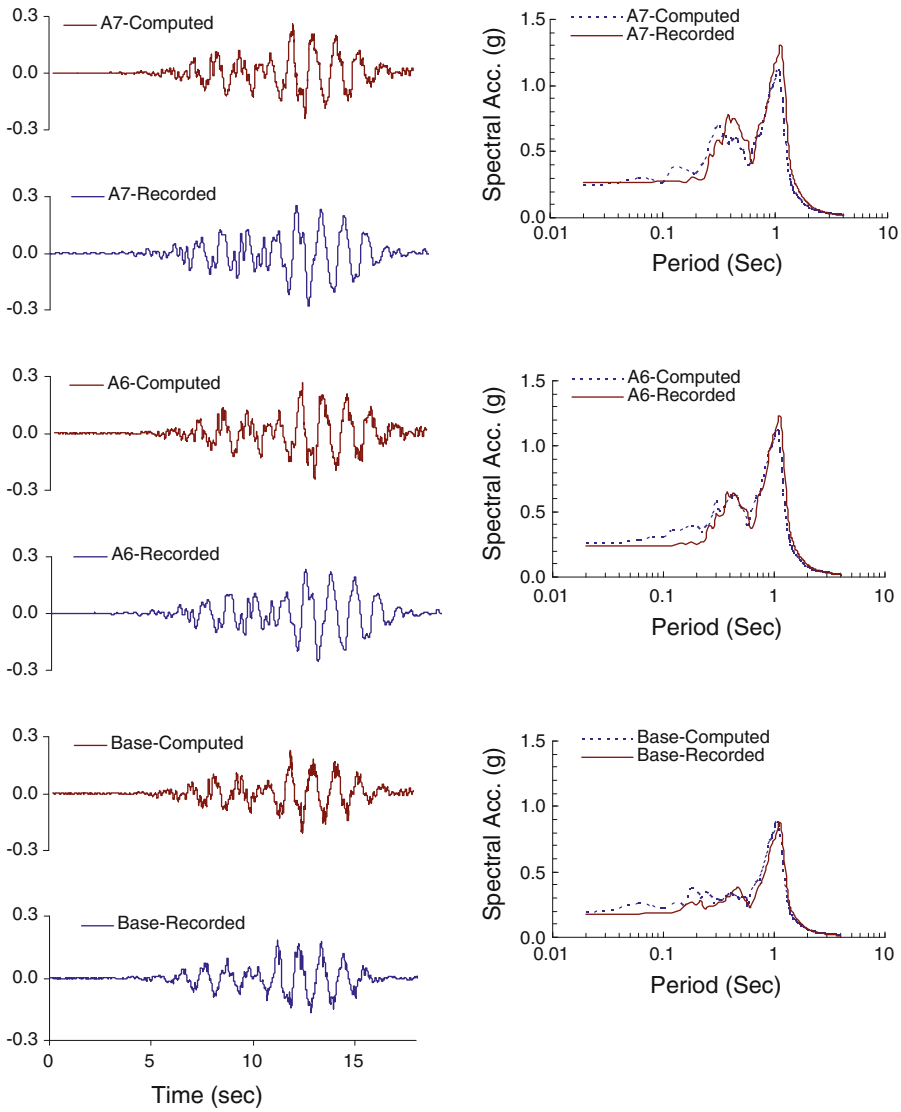

Fig. 10 Comparison between measured and predicted free field and beneath structure accelerations and response spectra of model RG-03 (WCM event)

shear wave velocity of 70 m/s and compared with those layered models. Figure 12 shows the response ratio of the foundation input motion (FIM) to free field (FF), in terms of acceleration, for all model during earthquake WCM ($a_{(max)} = 0.18$ g). It is noted that the response ratio for the uniform soil profile is much higher than those for layered profiles. It means that the foundation input motion demonstrates less amplification for layered profiles compared with uniform soil strata with the same average shear wave velocity. This indicates that soil layering could modify the unfavorable effects of SSI at the base of structure in earthquake prone area. Such behaviour was reported by Tokimatsu et al. (1996) for Kobe earthquake, in which the local site effects reduced the damage to superstructures located near coast lines.

The effect of inertial soil-structure interaction on structural response was assessed by comparing the structural response spectra to the response adjacent to the foundation. The deviation of the structure motion from the foundation motion is expressed by a transfer function that represents the ratio of structure and foundation motions in the frequency domain. Figure 13 shows the response spectra ratio of the structure to the response adjacent to the foundation in all models during the WCM event ($a_{(max)} = 0.18$ g). It can be seen that the peak response ratio for the structure is up to 34% higher than that of foundation input motion,

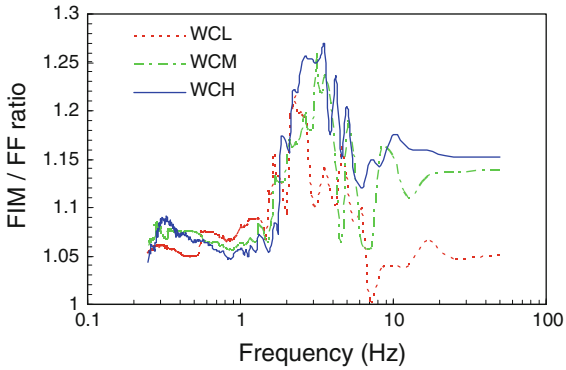

Fig. 11 Response spectra ratio ($SA_{FIM}/SA_{\text{Free field}}$) for three horizontal shaking events applied to model RG-03

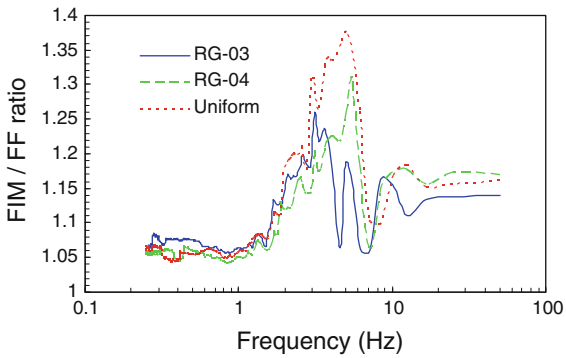

Fig. 12 Response spectra ratio ($SA_{FIM}/SA_{\text{Free field}}$) for three different models

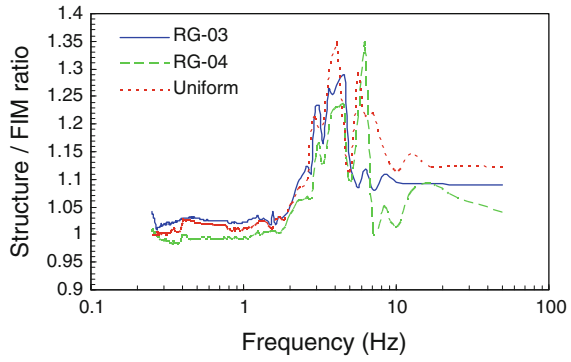

Fig. 13 Response spectra ratio of structure to foundation in all models for WCM event

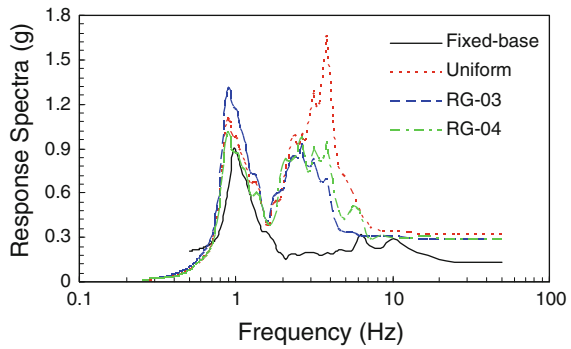

Fig. 14 Response spectra of structure on fixed-base and on different soil profile

which could be due to the effect of inertial SSI on structural response. Results also indicate that soil layering probably has negligible effect on modifying the inertial soil-structure interaction.

A series of analyses was also performed on fixed-base structure and its response was compared with response of the structure on different soil profiles to evaluate the effect of SSI (both kinematic and inertial) on structural response. As it can be seen from Fig. 14, SSI amplified the fixed-base structural response up to 1.6 g in uniform soft soil during the shaking event of WCM ($a_{(max)} = 0.18$ g). Soil-structure interaction also increased the natural period of the structure from about 0.15 s for fixed-base to about 0.3 s for structure on soil profiles. It is also noted that, as discussed earlier, the soil layering modified the peak structural response from about 1.66 g to about 0.95 g at the frequency range of 2–6 Hz by reducing the unfavorable effects of seismic SSI. This observation underscores the importance of considering the soil layering when evaluating the foundation input motion and site response analysis.

5 Conclusions

Seismic centrifuge model tests were conducted on two layered clay soil profiles to investigate soil-structure interaction and dynamic response of foundation. Layered soil profiles were used to trace the transmission of earthquake input motions through the soil. It was seen that, in general, there was higher amplification in soil of weaker stiffness, especially for low earthquake input motions. The structural response was greatly influenced by the soil stratification and soil-structure interaction. The amplification and the predominant frequency of the surface accelerations decreased with an increase in earthquake intensity. These effects were attributed to the reduction in soil

stiffness and increase in its material damping as the earthquake amplitude increased.

A numerical model was also developed using a fully coupled nonlinear finite difference program (FLAC) to predict the seismic response of the centrifuge tests. The numerical model was verified by comparing its predictions with the measured responses of two centrifuge model tests on layered clay. Comparison of results demonstrated a good agreement between the numerical simulations and centrifuge model recordings. The validated model was then used to study the effects of layering on earthquake amplification and soil-structure interaction.

The peak accelerations of soil beneath the structure increased due to strong interaction between the soil and the foundation. The seismic soil-structure interaction increased the horizontal ground motions at frequencies 2–6 Hz. Soil-structure interaction increased significantly both peak response and natural period of the fixed-base structure.

Soil layering was found to have a significant effect on foundation input motion. Soil layering modified the foundation input motion by reducing the unfavorable effects of SSI. These observations demonstrate the importance of considering the soil layering when evaluating the foundation input motion. However, inertial SSI analyses on different soil profile showed that soil layering has negligible effect on modifying the inertial SSI.

References

Aviles J, Perez-Rocha LE (1997) Site effects and soil-structure interaction in the Valley of Mexico. J Soil Dyn Earthq Eng 17:29–39

Bonilla MG (1991) Natural and artificial deposits in the Marina District, Chap. A of Effects of the Loma Prieta earthquake on the Marina District, San Francisco, California. U.S. Geological Survey Open- File Report 90-253, pp A1–A24

Bransby MF, Newson TA, Brunning P, Davies MCR (2001) Numerical and centrifuge modelling of the upheaval resistance of buried pipelines. In: Proceedings of OMAE pipeline symposium, Rio de Janeiro

Coulter SE, Phillips R (2003). Simulating submarine slope instability initiation using centrifuge model testing. In: Paper ISSMM-062 1st international symposium on submarine mass movements and their consequences, EGS-AGU-EUG joint assembly meeting, Nice, Kluwer Academic Publishers, The Netherlands

Crouse CB, Ramirez JC (2003) Soil-structure interaction and site response at the Jensen filtration plant during the 1994 Northridge, California, Main shock and Aftershocks. Bull Seismol Soc Am 93(2):546–556

Fox PJ, Lee J, Tong Q (2005) Model for large strain consolidation by centrifuge. Int J Geomech 5(4):267–275

Ghosh B, Madabhushi SPG (2003) Effect of localized soil inhomogenity in modifying seismic soil structure interaction. In: Proceeding of ASCE 16th engineering mechanics conference, Seattle, 16–18th July 2003, pp 1–8

Holzer T, Bennett M, Ponti D (1999) Liquefaction and soil failure during 1994 Northridge Earthquake. J Geotech Eng Div ASCE 126(6):438–452

Itasca (2005) FLAC3D: fast lagrangian analysis of continua in 3 dimensions, version 3.0, User Manual. Itasca Consulting Group, Inc., Minneapolis

Kutter BL, et al (1994) Design of a large earthquake simulator at UC Davis. In: Proceedings of cenrifuge'94, international conference on centrifuge modelling, Singapore

Randolph MG, Houlsby GT (1984) The limiting pressure on a circular pile loaded laterally in cohesive soil. Geotechnique 34(4):613–623

Rayhani MHT, El Naggar MH (2008a) Characterization of glyben for seismic application. Geotech Test J ASTM 31(1), paper ID: GTJ100552

Rayhani MHT, El Naggar MH (2008b) Numerical modeling of seismic response of rigid foundation on soft soil. Int J Geomech ASCE, November/December 336–346

Sanchez-sesma FJ (1987) Site effects on strong ground motion. J Soil Dyn Earthq Eng 6:124–132

Seid-Karbasi M (2003) Input motion time histories for dynamic testing in the c-core centrifuge facilities. Report no. 2003/01, University of British Columbia

Tokimatsu K, Mizuno H, Kakurai M (1996) Building damage associated with geotechnical problems. Special issue of soils and foundations, pp 219–234

Veletsos AS, Prasad AM (1989) Seismic interaction of structures and soils: stochastic approach. J Struct Eng ASCE 115(4):935–956